Supporting Information

Ammonia-mediated bromate inhibition during ozonation promotes the toxicity due to organic byproduct transformation

Qian-Yuan Wu[a], Lu-Lin Yang[a], Xin-Yang Zhang[a], Wen-Long Wang[b], Yao Lu[c], Ye Du[c,*], Yun-Lu[b], Hong-Ying Hu[b,c]

[a]Key Laboratory of Microorganism Application and Risk Control of Shenzhen, Guangdong Provincial Engineering Research Center for Urban Water Recycling and Environmental Safety, Tsinghua Shenzhen International Graduate School, Tsinghua University, Shenzhen 518055, China

[b]Environmental Simulation and Pollution Control State Key Joint Laboratory, State Environmental Protection Key Laboratory of Microorganism Application and Risk Control (SMARC), School of Environment, Tsinghua University, Beijing 100084, China

[c]Shenzhen Environmental Science and New Energy Technology Engineering Laboratory, Tsinghua-Berkeley Shenzhen Institute, Shenzhen 518055, China

Corresponding author:

Ye Du

Add: Tsinghua-Berkeley Shenzhen Institute, Shenzhen 518055, China

Tel: (+86-755) 2603-6326

Email: duyeah@sz.tsinghua.edu.cn

Number of pages: 24

Number of schemes: 1

Number of Tables: 4

Number of figures: 5

Text S1 Chemicals and reagents

For chemical analysis, ultrapure water (18.2 MΩ·cm) was prepared by a water purifier system (Milli-Q Integral). Ammonium chloride labeled with ^{15}N ($^{15}NH_4Cl$, ≥99%), ammonium chloride (NH_4Cl, ≥99.5%), potassium bromate ($KBrO_3$, ≥99.8%), potassium bromide (KBr, ≥99%), and potassium nitrate (KNO_3, ≥99%), were purchased from Sigma-Aldrich (St. Louis, MO, USA). All the solvents including methanol, acetone, and dichloromethane were of chromatographic grade and bought from MallinckrodtBaker Inc. (Phillipsburg, NJ, USA). Tannic acid (analytical reagent), gallic acid (99%), salicylic acid (99%), and vanillin (99%) were purchased from Aladdin (Shanghai, China). Suwannee River natural organic matter (SRNOM, 2R101N) was purchased from International Humic Substances Society.

For toxicity assays, phenol (99%), 4-nitroquinoline *N*-oxide (4-NQO, ≥98%), Hoechst 33342 (≥98%), and paraformaldehyde (95%) were obtained from Sigma-Aldrich (St. Louis, MO, USA). Triton X-100 (reagent grade) was purchased from Solarbio (Beijing, China). Dimethyl sulfoxide (DMSO, ≥99.7%), phosphate-buffered saline (Hyclone), and a mixture of Dulbecco's Modified Eagle Medium and F-12 (DMEM/F-12 1:1 medium) were bought from Thermo Fisher Scientific (Waltham, MA, USA). Bovine serum albumin (BSA) was purchased from Amresco (Solon, OH, USA). The kit for cytotoxicity assay (Cell Counting Kit-8, CCK-8) was obtained from Dojindo (Kumamoto, Japan). Primary antibody phospho-Histone H2AX and secondary antibody Alexa Fluor 647 conjugate for genotoxicity assay were purchased from Cell Signaling Technology (Boston, MA, USA).

Text S2 Br-N-DBP analysis and calculation of their cytotoxicity index and genotoxicity index

Haloacetonitriles were analyzed by GC-ECD (7890B, Agilent Technologies, USA) equipped with a DB-5MS capillary column (30 m × 0.25 mm × 0.25 μm, Agilent, USA). Injections of 1 μL of the extracts were introduced via a splitless injector using nitrogen as the carrier gas. The injector and detector temperatures were 230 and 250 °C, respectively. The initial column temperature was 35 °C (maintained for 3 min), which was increased to 70 ℃ at a rate of 20 °C/min (maintained for 1 min), then 90 °C at a rate of 5 °C/min (maintained for 1 min), then 160 °C at a rate of 20 °C/min (maintained for 1 min), and finally 220 °C at a rate of 40 °C/min (maintained for 3 min).

Halonitromethanes were analyzed by GC-ECD (7890B, Agilent Technologies, USA) equipped with a DB-5MS capillary column (30 m × 0.25 mm × 0.25 μm, Agilent, USA). Injections of 1 μL of the extracts were introduced via a splitless injector using nitrogen as the carrier gas. The injector and detector temperatures were 117 and 250 °C, respectively. The initial column temperature was 35 °C (maintained for 6 min), which was increased to 190 ℃ at a rate of 20 °C/min (maintained for 5 min). The relatively low injector temperature was used to prevent the thermal decomposition of tribromonitromethanes (Hong et al., 2013; Plewa et al., 2004).

Haloacetamides were analyzed by GC-ECD equipped with a Rtx-1701 capillary column (30 m × 0.25 mm × 0.25 μm, RESTEK, USA). Injections of 1 μL of the extracts were introduced via a splitless injector using nitrogen as the carrier gas. The injector and detector temperatures were 230 and 250 °C, respectively. The initial column

temperature was 35 °C (maintained for 3 min), which was increased to 90 °C at a rate of 20 °C/min (maintained for 1 min), then 160 °C at a rate of 20 °C/min (maintained for 1 min), and finally 220 °C at a rate of 40 °C/min (maintained for 5 min).

Contributions of these Br-N-DBPs to cytotoxicity and genotoxicity were estimated using the cytotoxicity index (CTI) and genotoxicity index (GTI), according to the method of Chuang et al. (2019) using previously reported LC_{50} (for cytotoxicity) and EC_{50} (for genotoxicity) values based on CHO cells (Wagner and Plewa, 2017). CTI and GTI were calculated using Eqs. (1) and (2). A smaller toxicity index means less contribution of the corresponding DBP to toxicity.

$$\text{CTI} = \text{DBP concentration}/LC_{50} \quad (1)$$

$$\text{GTI} = \text{DBP concentration}/EC_{50} \quad (2)$$

Text S3 Cell culture

The CHO-k1 cell line purchased from the American Type Culture Collection was used to perform the toxicity assay. The culture medium DMEM/F12 (1:1) was added with streptomycin (0.1 mg/mL), penicillin G (100 unit/mL), and fetal bovine serum (10%). Cells culture dishes were placed in an incubator with saturated humidity and 5% CO_2 gas at 37 °C. Cells undergoing 2–5 passages were used for the toxicity assay. Cell passaging was conducted every 48 h.

Text S4 Cytotoxicity assay and cytotoxicity equivalent quantification

To perform cytotoxicity assay, 1×10^4 cells per well were seeded in a sterile 96-

well plate (3599, Corning, USA), and cultured for 12 h before the cells were exposed to organic byproducts. The dried organic extracts were firstly dissolved in DMEM/F12 containing 0.5% DMSO (v:v), then further diluted to 6-8 different concentration factors by DMEM/F12 containing 0.5% DMSO. Cell cultures were exposed to the solution for 48 h. DMEM/F12 containing 0.5% DMSO was used as the negative control, while phenol dissolved in DMEM/F12 containing 0.5% DMSO was used as the reference compound. All the 96-well plates for toxicity assay were covered with the sterilized seal films to avoid the cross contamination. After 48 h exposure, the culture medium was discarded. Cells were washed with 100 μL phosphate buffered solution (PBS). Then 100 μL of the reagent in Cell Counting Kit-8 (CCK-8) dissolved in DMEM/F12 was added into each well of the 96-well plates. Cells were then cultured in the incubator (37 °C) for another 2 h, then the absorbance of each well at 450 nm was measured using the microplate reader SpectraMax i3 (Molecular Devices, USA). Each test was performed in 6-12 replicates.

The cell viability (CV) for a sample or reference compound was calculated according to Eq. (1):

$$CV=(A_S-A_B)\ /(A_N-A_B), \quad (1)$$

where CV is the cell viability for a sample or phenol against the negative control. The A_S is the absorbance of the sample or phenol at 450 nm. A_B is the absorbance of the blank control (only added the Cell Counting Kit-8 reagent dissolved in DMEM/F12) at 450 nm. The A_n is the absorbance of the negative control at 450 nm.

The CV values at different concentration factors of each sample were used to

create a concentration–effect curve. Similarly, concentration–effect curve of phenol was obtained with the CV values at different concentrations. The concentration at which the CV value was 50% from the regression analysis was defined as the lethal concentration of 50% (LC_{50}). The cytotoxicity equivalent of a sample was calculated according to Eq. (2):

$$\text{Cytotoxicity equivalent}=LC_{Phenol,50}/LC_{Sample,50} \quad (2)$$

where the cytotoxicity equivalent unit is mg–phenol/L. $LC_{Phenol,50}$ is the LC_{50} of the reference compound phenol. $LC_{sample,50}$ is the LC_{50} of a sample.

Text S5 DNA DSB assay and genotoxicity equivalent quantification

To perform the genotoxicity assay, 5×10^3 cells were seeded in each well of sterile 96-well plate (3603, Corning, USA), pre-cultured for 12 h, and exposed to organic byproducts dissolved in DMEM/F12 containing 0.5% DMSO at 6-8 concentrations. DMEM/F12 containing 0.5% DMSO was used as the negative control, while 4-nitroquinoline *N*-oxide (4-NQO) dissolved in DMEM/F12 containing 0.5% DMSO was used as the reference compound. All the 96-well plates for toxicity assay were covered with the sterilized seal films to avoid the cross contamination. The 6-12 replicates of each test were performed. After exposure for 24 h, cells were fixed with paraformaldehyde, permeated with Triton-100, and blocked with bovine serum albumin. Cells were incubated with the primary antibody phospho-histone H2AX and then stained with the second antibody Alexa Fluor® 647 conjugate together with Hoechst 33258. After the staining, images of the cells were obtained using an HCA system (ImageXpress® Micro, Molecular Devices, USA) with a 40× objective lens. The

pH2AX foci were obtained from the CY5 channel and nucleus DNA was obtained from the DAPI channel. In each well of the plate, the number of pH2AX per cell was calculated by the total number of pH2AX foci over the number of nucleus.

The pH2AX induction rate of a sample was calculated according to Eq. (3):

$$IR=(\text{pH2AX foci per cell})_s/(\text{pH2AX foci per cell})_n \quad (3)$$

where IR is the pH2AX foci induction ratio for a sample or 4-NQO against the negative control. The $(\text{pH2AX foci per cell})_s$ is the number of pH2AX foci induced by a sample or 4-NQO. The $(\text{pH2AX foci per cell})_n$ is the number of pH2AX foci induced by the negative control. The pH2AX foci induction ratios of samples at different concentration factors with cell viabilities >70% (Plewa et al., 2010) were used to obtain concentration–effect curves by regression analysis. The genotoxicity equivalent of a sample was calculated according to Eq. (4):

$$\text{Genotoxicity equivalent}=\frac{(IR_{1.5})_{4-NQO}}{(IR_{1.5})_{Sample}} \quad (4)$$

where the unit of genotoxicity equivalent is μg–4-NQO/L, $(IR_{1.5})_{4\text{-NQO}}$ is the concentration of the 4-NQO solution that leads to the 1.5-fold induction ratio over the negative control, and $(IR_{1.5})_{\text{Sample}}$ is the concentration of a sample that leads to the 1.5 fold induction ratio over the negative control.

Text S6 Rough calculation of the extent of HOBr/OBr- reduced by NH_4^+ or H_2O_2

It is difficult to model the whole process of SRNOM/O_3/Br^-/NH_4^+ or SRNOM/O_3/Br^-/ H_2O_2 because some critical information is unknown. For example, the rate constant of HOBr and SRNOM ($k_{\text{HOBr, SRNOM}}$) was not reported. Moreover, the $k_{\text{HOBr,}}$

$_{SRNOM}$ would vary during the ozonation process with the change of SRNOM property. Besides, the self-decomposition mechanism of $NHBr_2$, the rate constant of NH_2Br and SRNOM were also unknown. However, based on reasonable assumptions we can roughly understand to what extent HOBr/OBr^- concentration would be reduced by the addition of NH_4^+ or H_2O_2.

(1) In the SRNOM/Br^-/O_3/NH_4^+ system, taken the reaction condition of O_3 5 mg/L, Br^- 0.5 mg/L, NH_3 0.5 mg-N/L, NOM 5 mg-C/L as example.

The initial concentrations were $[O_3]$=5 mg/L, 1.04×10^{-4} M; $[Br^-]$=0.5 mg/L, 6.25×10^{-6} M; $[NH_3]_T$=0.5 mg-N/L, 3.57×10^{-5} M; [NOM]=5 mg-C/L, 4.17×10^{-4} M-C; $[H_2O_2]_T$=17 mg/L, 5×10^{-4} M. The distribution of HOBr and OBr^- could be calculated as:

$$HOBr \leftrightarrow H^+ + BrO^-,\ \text{pKa=8.7, pH=7.0} \rightarrow [BrO^-] = 0.02\bullet[HOBr]_T,\ [HOBr] = 0.98\bullet[HOBr]_T$$

HOBr would react with both O_3, ·OH, SRNOM and NH_3. The maximum concentration of O_3 and ·OH were assumed and the rate of each elementary reaction was expressed in Table S2. From Table S2 (reactions 1-6), even under the assumed maximum concentration of O_3 and ·OH, reactions of HOBr/ OBr^- and O_3/ ·OH (reactions 2, 3, 4 and 5) were negligible, while the reaction 1 (HOBr and SRNOM) and reaction 6 (HOBr and NH_3) would be prevailing.

The ratio of HOBr reacting with SRNOM was estimated as 186/(186+2800)*100%=6%, while the ratio of HOBr reacting with NH_3 was estimated as 2800/(186+2800)*100%=94%, namely 94% HOBr would be transformed to NH_2Br. The formed NH_2Br further reacts with O_3, ·OH, HOBr and SRNOM. Due to the

unknown mechanism and rate constant, it was not discussed here.

(2) In the SRNOM/Br^-/O_3/H_2O_2 system, taken the reaction condition of O_3 5 mg/L, Br^- 0.5 mg/L, H_2O_2 17 mg /L, NOM 5 mg-C/L as example.

The initial concentrations were $[O_3]$=5 mg/L, 1.04×10^{-4} M; $[Br^-]$=0.5 mg/L, 6.25×10^{-6} M; [NOM]=5 mg-C/L, 4.17×10^{-4} M; $[H_2O_2]_T$=17 mg/L, 5×10^{-4} M. The distribution of H_2O_2 and H_2O^- could be calculated as:

$H_2O_2 \leftrightarrow H^+ + H_2O^-$, pKa=11.75, pH=7.0 $\rightarrow [H_2O_2] = 0.99 \bullet [H_2O_2]_T$, $[H_2O^-] = 1.78\times10^{-5} \bullet [H_2O_2]_T$

HOBr would react with both O_3, ·OH, SRNOM and H_2O_2. From Table 1, among the involved reactions of 1-5, 18, 19, only reaction 1 (HOBr and SRNOM), reaction 18 (OBr^- and H_2O_2) and reaction 19 (HOBr and H_2O^-) would be prevailing. The ratio of HOBr reacting with SRNOM was estimated as 186/(186+650+6.8)*100%=22%, while the ratio of HOBr reacting with H_2O_2 was estimated as (650+6.8)/(186+650+6.8)*100%=78%, namely 78% HOBr would be suppressed by H_2O_2.

Pathway I (Direct/Indirect pathway):

$$Br^- \xrightarrow[k=160 M^{-1}\bullet s^{-1}]{O_3} HOBr / OBr^- \xrightarrow[\substack{k=4.5\times10^9 M^{-1}\bullet s^{-1} \text{ for } OBr^- \\ k=2\times10^9 M^{-1}\bullet s^{-1} \text{ for HOBr}}]{\bullet OH} BrO\bullet \xrightarrow[k=5\times10^9 M^{-1}\bullet s^{-1}]{BrO\bullet} BrO_2^- \xrightarrow[k>10^5 M^{-1}\bullet s^{-1}]{O_3} BrO_3^-$$

Pathway II (Direct pathway):

$$Br^- \xrightarrow[k=160 M^{-1}\bullet s^{-1}]{O_3} HOBr / OBr^- \xrightarrow[\substack{k=100 M^{-1}\bullet s^{-1} \text{ for } OBr^- \\ k\le0.013 M^{-1}\bullet s^{-1} \text{ for HOBr}}]{O_3} BrO_2^- \xrightarrow[k>10^5 M^{-1}\bullet s^{-1}]{O_3} BrO_3^-$$

Pathway III (Indirect/ Direct pathway):

$$Br^- \xrightarrow[k=1.1\times10^9 M^{-1}\bullet s^{-1}]{OH\bullet} Br\bullet \xrightarrow[k=1.5\times10^8 M^{-1}\bullet s^{-1}]{O_3} BrO\bullet \xrightarrow[k=5\times10^9 M^{-1}\bullet s^{-1}]{BrO\bullet} BrO_2^- \xrightarrow[k>10^5 M^{-1}\bullet s^{-1}]{O_3} BrO_3^-$$

Scheme S1 Simplified pathways for bromate formation during ozonation (Adapted from Buxton et al. (1988), Haag and Hoigné, (1983), Hofmann and Andrews (2006), Song et al., (1996), von Gunten and Hoigne (1994))

Table S1 Reactions and rate constants during ozonation of water containing bromide in the presence of ammonia or hydrogen peroxide

No.	Reaction	k (25 °C)	Reference
R1	$HOBr + NH_3 \rightarrow NH_2Br$	k_1=8×10^7 M^{-1}·s^{-1}	Haag et al., 1984
R2	$NH_2Br + OBr^- + OH^- \rightarrow N_2 + Br^- + H_2O$	k_2=0.1~4.7×10^{-4} s^{-1}	Hofmann and Andrews, 2001
R3	$NH_2Br + HOBr \rightarrow NHBr_2$	k_3=7.0×10^5 M^{-1}·s^{-1}	Haag and Lietzke, 1980
R4	$NHBr_2 + HOBr \rightarrow NBr_3$	k_4=2.5×10^4 M^{-1}·s^{-1}	Haag and Lietzke, 1980
R5	$NH_2Br + O_3 \rightarrow Br^- + NO_3^-$	k_5=40 M^{-1}·s^{-1}	von Gunten and Hoigne, 1994
R6	$NHBr_2 + O_3 \rightarrow Br^- + NO_3^-$	k_6=10 M^{-1}·s^{-1}	von Gunten and Hoigne, 1994
R7	$OBr^- + H_2O_2 \rightarrow Br^- + H_2O + O_2$	k_7=1.3 ×10^6 M^{-1}·s^{-1}	von Gunten and Oliveras, 1997
R8	$HOBr + HO_2^- \rightarrow Br^- + H_2O + O_2$	k_8=7.6 ×10^8 M^{-1}·s^{-1}	von Gunten and Oliveras, 1997
R9	$HOBr + NOM \rightarrow products$	k_9=4.56×10^5 M^{-1}·s^{-1} [a]	Duirk and Valentine, 2007

Note:

[a] The k value was obtained from a river water located in Iowa, the U.S.A., not SRNOM (Duirk and Valentine, 2007).

Table S2 Assumed reaction rate during ozonation of water containing bromide in the presence of ammonia or hydrogen peroxide

No.	Reaction	*k*	Assumed maximum conc. (M)	Rate expression	Assumed maximum reaction rate	Reference
1	$HOBr + NOM \rightarrow products$	4.56×10^{5} $M^{-1}\cdot s^{-1}$ a	[NOM] 4.17×10^{-4}	k[NOM][HOBr]	$1.86\times10^{2}\cdot$ $[HOBr]_T$	Duirk and Valentine, 2007
2	$HOBr + O_3 \rightarrow BrO_2^- + O_2 + H^+$	0.013 $M^{-1}\cdot s^{-1}$	$[O_3]$ 1.04×10^{-4}	$k[O_3][HOBr]$	$1.32\times10^{-6}\cdot$ $[HOBr]_T$	Haag and Lietzke, 1980
3	$OBr^- + O_3 \rightarrow BrO_2^- + O_2$	100 $M^{-1}\cdot s^{-1}$	$[O_3]$ 1.04×10^{-4}	$k[O_3][OBr^-]$	$2.08\times10^{-4}\cdot$ $[HOBr]_T$	Haag and Lietzke, 1980
4	$HOBr + \bullet OH \rightarrow BrO\bullet + H_2O$	2×10^{9} $M^{-1}\cdot s^{-1}$	$[\cdot OH]$ 1.0×10^{-11} b	$k[\cdot OH][HOBr]$	$1.96\times10^{-2}\cdot$ $[HOBr]_T$	Buxton et al., 1988
5	$OBr^- + \bullet OH \rightarrow BrO\bullet + OH^-$	4.5×10^{9} $M^{-1}\cdot s^{-1}$	$[\cdot OH]$ 10^{-11}	$k[\cdot OH][OBr^-]$	$9.0\times10^{-4}\cdot$ $[HOBr]_T$	Buxton et al., 1988
6	$HOBr + NH_3 \rightarrow NH_2Br$	8×10^{7} $M^{-1}\cdot s^{-1}$ c	$[NH_3]$ 3.57×10^{-5}	$k[NH_3][HOBr]$	$2.80\times10^{3}\cdot$ $[HOBr]_T$	Wajon and Morris, 1982
7	$NH_3 + 4O_3 \rightarrow H^+ + NO_3^- + H_2O + 4O_2$	5 $M^{-1}\cdot s^{-1}$	$[NH_3]$ 3.57×10^{-5} $[O_3]1.04\times10^{-4}$	k[NOM][HOBr]	3.64×10^{-9} $M\cdot s^{-1}$	Haag et al., 1984
8	$NH_2Br + O_3 \rightarrow Br^- + NO_3^-$	40 $M^{-1}\cdot s^{-1}$	\	\	\	von Gunten and Hoigne, 1994
9	$NH_2Br + NOM \rightarrow products$	*unknown*	\	\	\	\
10	$NH_2Br + OBr^- + OH^- \rightarrow N_2 + Br^- + H_2O$	1×10^{-5} s^{-1}	\	\	\	Hofmann and Andrews, 2001
11	$NH_2Br + HOBr \rightarrow NHBr_2$	$k_3=7.0\times10^{5}$ $M^{-1}\cdot s^{-1}$	\	\	\	Haag and Lietzke, 1980

12	$NHBr_2 + NOM \rightarrow products$	*unknown*	\	\	\	\
13	$NHBr_2$ decay, *unknown*	*unknown*	\	\	\	Hofmann, 2000
14	$NHBr_2 + O_3 \rightarrow Br^- + NO_3^-$	10 $M^{-1}\cdot s^{-1}$	\	\	\	von Gunten and Hoigne, 1994
15	$NHBr_2 + HOBr \rightarrow NBr_3$	2.5×10^4 $M^{-1}\cdot s^{-1}$	\	\	\	Haag and Lietzke, 1980
16	$2NBr_3 + 3H_2O \rightarrow N_2 + 3HOBr + 3H^+ + 3Br^-$	*unknown*	\	\	\	Hofmann, 2000
17	$NBr_3 + NOM \rightarrow products$	*unknown*	\	\	\	\
18	$OBr^- + H_2O_2 \rightarrow Br^- + H_2O + O_2$	1.3×10^6 $M^{-1}\cdot s^{-1}$	$[H_2O_2]$ 5×10^{-4}	$k[H_2O_2][HOBr]$	$6.5\times10^2\cdot[HOBr]_T$	von Gunten and Oliveras, 1997
19	$HOBr + HO_2^- \rightarrow Br^- + H_2O + O_2$	7.6×10^8 $M^{-1}\cdot s^{-1}$	$[H_2O^-]$ 8.9×10^{-9}	$k[H_2O^-][HOBr]$	$6.8\cdot[HOBr]_T$	von Gunten and Oliveras, 1997

Note:

[a] The *k* value was obtained from a river water located in Iowa, the U.S.A., not SRNOM (Duirk and Valentine, 2007).

[b] The steady state concentration of ·OH was assumed according to the data from a SRNOM/O_3 system (DOC 4 mg-C/L, O_3 4 mg/L, reaction time 180 s) reported previously (Wang et al., 2020), of which the condition was similar to this study. The ·OH exposure ($\int[\cdot OH]dt$) and the steady state concentration of ·OH ($[\cdot OH]_{ss}$) could be calculated according to equation (1) and (2):

$$\int[\bullet OH]dt = R_{\cdot OH,O_3} \bullet \Delta[O_3]_t \quad (1)$$

$$[\cdot OH]_{ss} = \int[\cdot OH]dt/t \quad (2)$$

Where $R_{\cdot OH, O_3}$ is the $\int[\bullet OH]dt$ per unit of O_3 consumed (5.10×10^{-6} s); $\Delta[O_3]t$ is the consumed O_3 (4 mg/L, 8.33×10^{-5} M); *t* is the reaction time (180 s). The $[\cdot OH]_{ss}$ is therefore calculated as $2.36\times10^{-}$

[12] M. Here the maximum concentration of [·OH] was assumed as 1.0×10^{-11} M. Moreover, the assumed maximum concentration of 1.0×10^{-11} M would also be applicable in the O_3/H_2O_2 system (Rosenfeldt et al., 2006).

[c] The *k* value was obtained using the concentration of total ammonia (Wajon and Morris, 1982). Therefore, the distribution of NH_4^+ and NH_3 was not considered.

Table S3 Concentrations of Br-N-DBPs formed during ozonation and their cytotoxicity index (CTI) and genotoxicity index (GTI)[a]

DBPs	Cyto-toxicity LC_{50} (M)[b]	Geno-toxicity EC_{50} (M)[c]	Concentration (M)		CTI		GTI	
			Br^-	Br^- and NH_4^+	Br^-	Br^- and NH_4^+	Br^-	Br^- and NH_4^+
MBAN	3.21×10^{-6}	3.85×10^{-5}	1.62×10^{-9}	9.58×10^{-10}	5.05×10^{-4}	2.98×10^{-4}	4.21×10^{-5}	4.21×10^{-5}
DBAN	2.85×10^{-6}	4.71×10^{-5}	6.28×10^{-10}	\	2.20×10^{-4}	\	1.33×10^{-5}	\
DBNM	6.09×10^{-6}	2.62×10^{-5}	\	9.36×10^{-10}	\	1.53×10^{-4}	\	7.06×10^{-5}
TBNM	8.57×10^{-6}	6.99×10^{-5}	1.11×10^{-9}	1.61×10^{-9}	1.30×10^{-4}	1.88×10^{-4}	1.59×10^{-5}	2.30×10^{-5}
MBAcAm	1.89×10^{-6}	3.68×10^{-5}	\	2.39×10^{-9}	\	1.26×10^{-3}	\	6.49×10^{-5}
DBAcAm	1.22×10^{-5}	7.44×10^{-4}	\	6.22×10^{-10}	\	5.10×10^{-5}	\	8.36×10^{-7}
TBAcAm	3.14×10^{-6}	3.25×10^{-5}	\	4.22×10^{-10}	\	1.34×10^{-4}	\	1.30×10^{-5}
Sum	\	\	\	\	8.55×10^{-4}	2.08×10^{-3}	7.13×10^{-5}	2.14×10^{-4}

[a] The experiment conditions are O_3 5 mg/L, Br^- 0.5 mg/L, NH_4^+–N 0.5 mg/L.

[b] LC_{50} values are cited from Wagner and Plewa (2017).

[c] EC_{50} values are cited from Wagner and Plewa (2017).

Table S4 Cytotoxicity index (CTI) and genotoxicity index (GTI) of Br-N-DBPs at the concentration factor of the measured LC_{50} or $IR_{1.5}$ in this study

Experimental conditions	O_3 5 mg/L, Br^- 0.5 mg/L		O_3 5 mg/L, Br^- 0.5 mg/L, NH_4^+–N 0.5 mg/L	
	Cytotoxicity	Genotoxicity	Cytotoxicity	Genotoxicity
Measured LC_{50} or $IR_{1.5}$ in this study (folds)	297	134	189	78
CTI or GTI at the concentration factor of 1	8.55×10^{-4}	7.13×10^{-5}	2.08×10^{-3}	2.14×10^{-4}
CTI or GTI at the concentration factor of the measured LC_{50} or $IR_{1.5}$	0.25	0.010	0.39	0.016

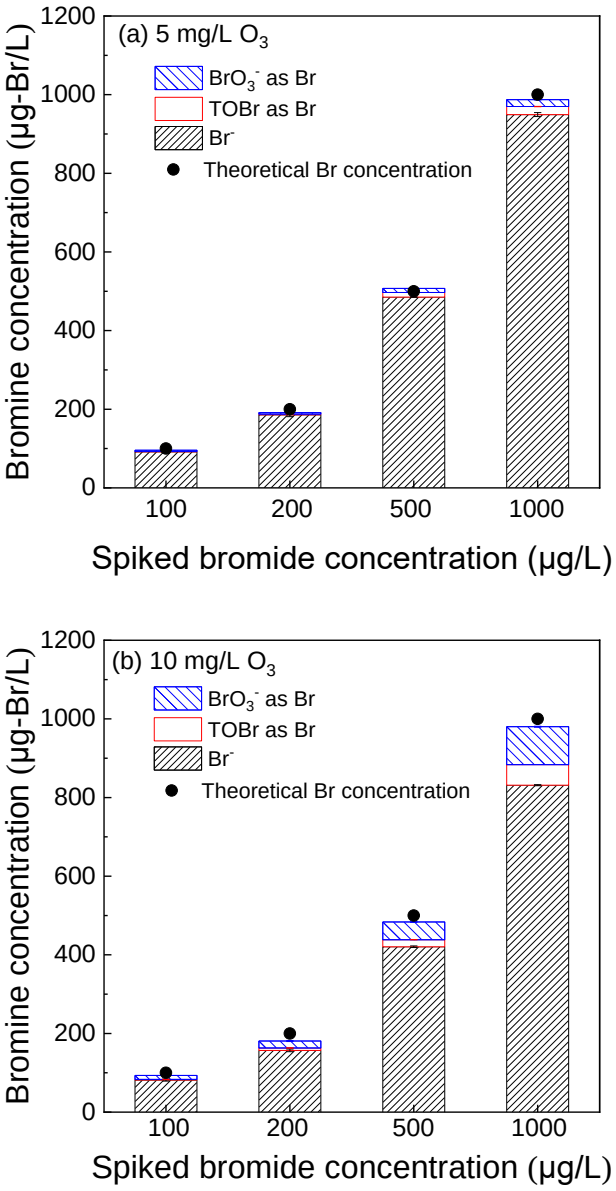

Figure S1 Mass balance of bromine during ozonation: **(a)** Ozone dose 5 mg/L; **(b)** Ozone dose 10 mg/L

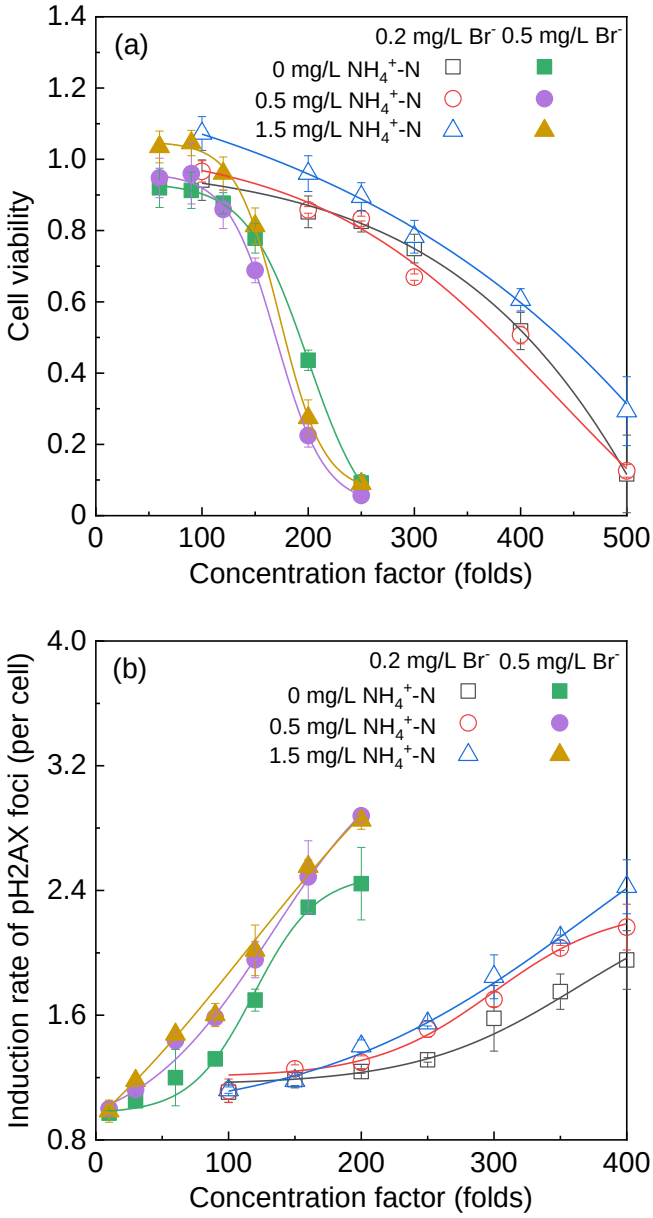

Figure S2 Influence of ammonia on the toxicity of organic byproducts formed during ozonation in the presence of bromide: **(a)** Concentration-effect curves in the cytotoxicity assay (ozone dose 10 mg/L); **(b)** Concentration-effect curves in the genotoxicity assay (ozone dose 10 mg/L)

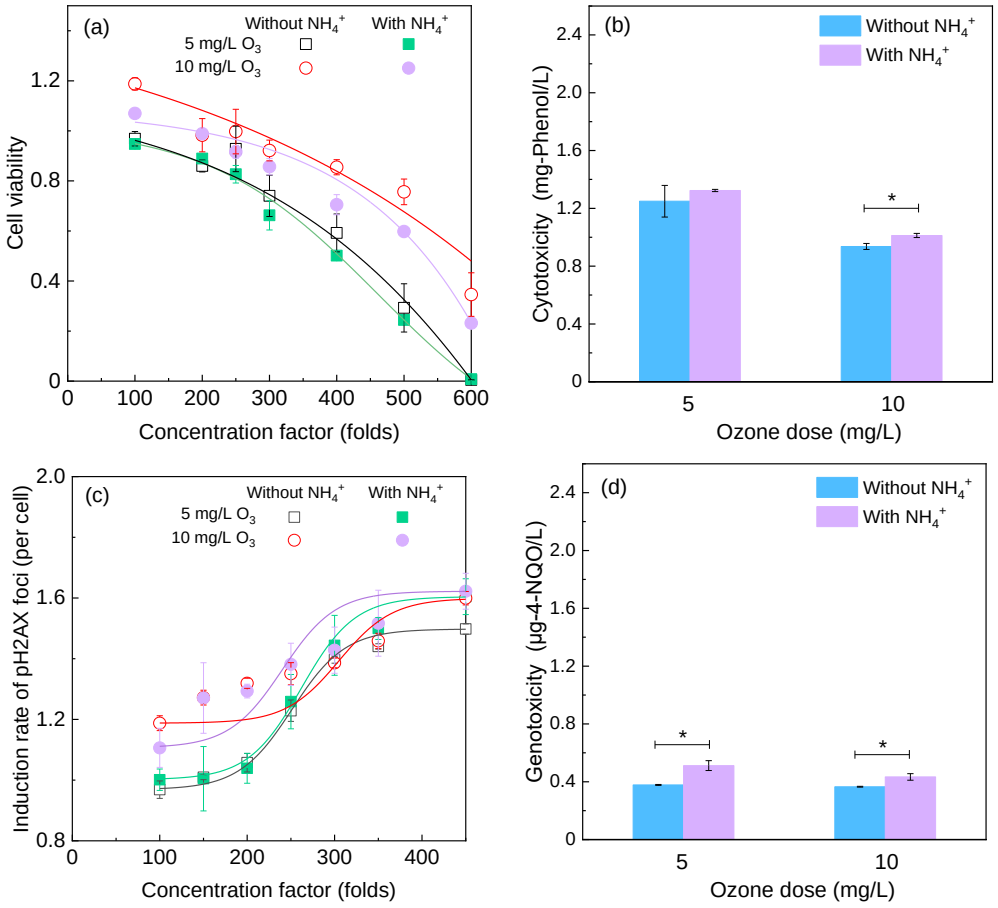

Figure S3 Influence of ammonia on the toxicity during ozonation in the absence of bromide (NH_4^+-N 1.5 mg/L): **(a)** Concentration-effect curves in the cytotoxicity assay; **(b)** Cytotoxicity equivalents (* indicates significantly increased cytotoxicity from the addition of ammonia compared to that without adding ammonia; one-way ANOVA, $p<0.05$); **(c)** Concentration-effect curves in the genotoxicity assay; **(d)** Genotoxicity equivalents (* indicates significantly increased genotoxicity from the addition of ammonia compared to that without adding ammonia; one-way ANOVA, $p<0.05$).

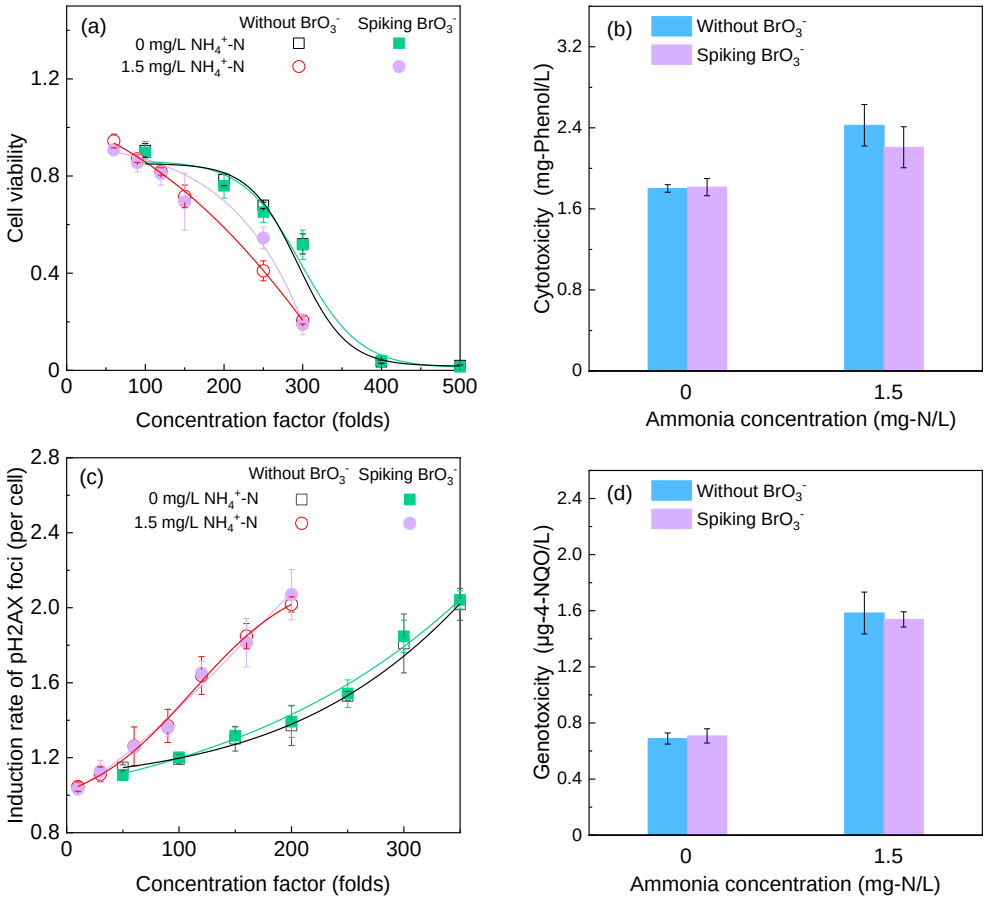

Figure S4 Influence of the formed bromate on the toxicity of organic byproducts. (5 mg/L O_3, 0.5 mg/L Br^-. The formed bromate was measured and then spiked into the organic extracts by the same concentration factor as organic extracts. The formed bromate concentration were 16 μg/L (not adding ammonia) and 12 μg/L (adding 1.5 mg/L NH_4^+-N)): **(a)** Concentration-effect curves in the cytotoxicity assay; **(b)** Cytotoxicity equivalents; **(c)** Concentration-effect curves in the genotoxicity assay; **(d)** Genotoxicity equivalents.

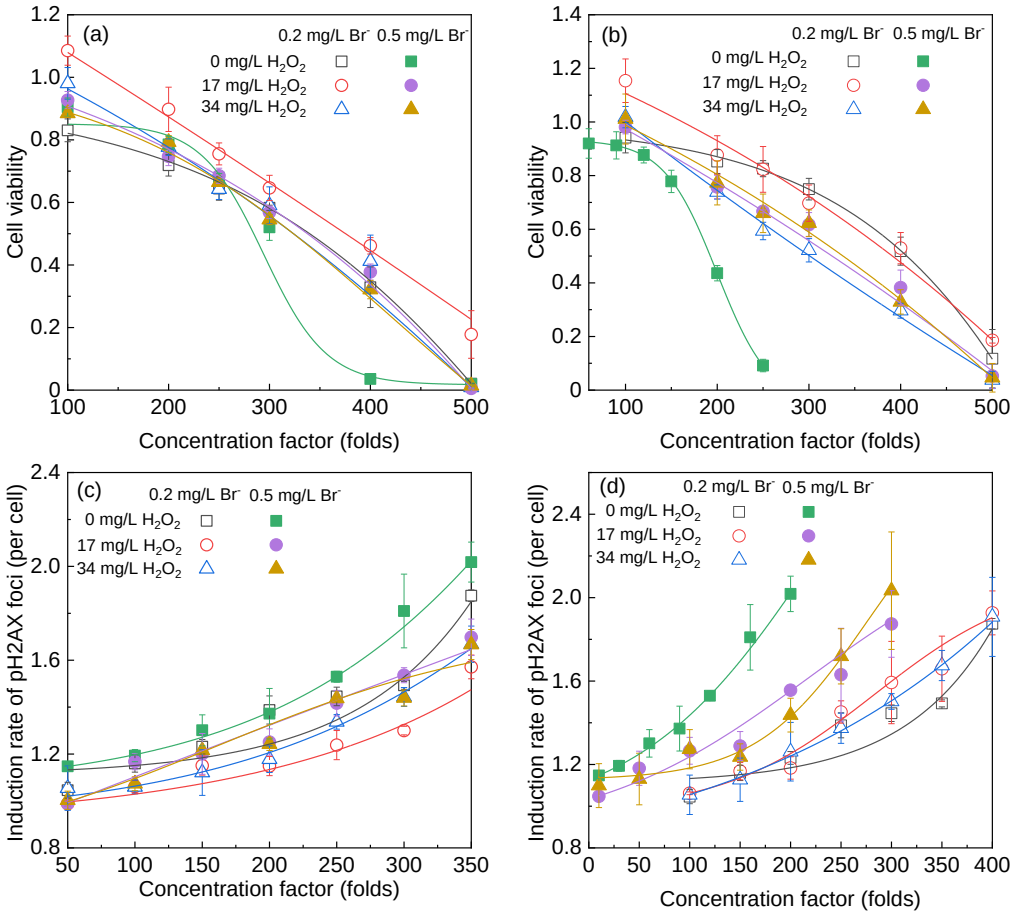

Figure S5 Influence of hydrogen peroxide (H_2O_2) on the toxicity of organic byproducts formed during ozonation in the presence of bromide: **(a)** Concentration-effect curves in the cytotoxicity assay (O_3 5 mg/L); **(b)** Concentration-effect curves in the cytotoxicity assay (O_3 10 mg/L); **(c)** Concentration-effect curves in the genotoxicity assay (O_3 5 mg/L); **(d)** Concentration-effect curves in the genotoxicity assay (O_3 10 mg/L)

References

Berne, F., Chasson, G., Legube, B. Effect of addition of ammonia on the bromate formation during ozonation. *Ozone: Science and Engineering*, **2004**, *26*(3), 267-276.

Buxton, G. V.; Greenstock, C. L.; Helman, W. R.; Ross, A. B. Critical review of rate constants for reactions of hydrated electrons, hydrogen atoms and hydroxyl radicals ($\cdot OH/\cdot O^-$) in aqueous solution. J. Phys. Chem. Ref. Data **1988**, *17*, 513-886.

Chuang, Y. H., Szczuka, A., Mitch, W. A. Comparison of toxicity-weighted disinfection byproduct concentrations in potable reuse waters and conventional drinking waters as a new approach to assessing the quality of advanced treatment train waters. *Environ. Sci. Technol*. **2019**, *53*, 3729-3738.

Duirk, S. E.; Valentine, R. L. Bromide oxidation and formation of dihaloacetic acids in chloraminated water. *Environ. Sci. Technol.* **2007**, *41*(20), 7047-7053.

Haag, W. R.; Hoigné, J.; Bader, H. Improved ammonia oxidation by ozone in the presence of bromide ion during water treatment. *Water Res.* **1984**, *18* (9), 1125-1128.

Haag, W. R.; Lietzke, M. H. Kinetic model for predicting the concentrations of active halogens species in chlorinated saline cooling waters. Final report (No. ORNL/TM-7942). *Oak Ridge National Lab., TN (USA).* **1981**.

Hofmann, R. Using ammonia to inhibit bromate formation during ozonation. Doctoral dissertation, National Library of Canada, 2000.

Hofmann, R.; Andrews, R. C. Ammoniacal bromamines: a review of their influence on bromate formation during ozonation. *Water Res.* **2001**, *35* (3), 599-604.

Hofmann, R.; Andrews, R. C. Impact of H_2O_2 and (bi)carbonate alkalinity on ammonia's inhibition of bromate formation. *Water Res.* **2006***, 40* (18), 3343-3348.

Hong, H., Xiong, Y., Ruan, M., Liao, F., Lin, H., Liang, Y. Factors affecting THMs, HAAs and HNMs formation of Jin Lan Reservoir water exposed to chlorine and monochloramine. *Sci. Total Environ.* **2013***, 444*, 196-204.

Plewa, M. J.; Simmons, J. E.; Richardson, S. D.; Wagner, E. D. Mammalian cell cytotoxicity and genotoxicity of the haloacetic acids, a major class of drinking water disinfection by-products. *Environ. Mol. Mutagen*. **2010,** *51* (8-9), 871-878.

Plewa, M. J., Wagner, E. D., Jazwierska, P., Richardson, S. D., Chen, P. H., McKague, A. B. Halonitromethane drinking water disinfection byproducts: chemical characterization and mammalian cell cytotoxicity and genotoxicity. *Environ. Sci. Technol.* **2004**, *38*(1), 62-68.

Rosenfeldt, E. J., Linden, K. G., Canonica, S., Von Gunten, U. Comparison of the efficiency of OH radical formation during ozonation and the advanced oxidation processes O_3/H_2O_2 and UV/H_2O_2. *Water Res.* **2006**, *40*(20), 3695-3704.

Song, R. Ozone–bromide–NOM interactions in water treatment. University of Illinois at Urbana-Champaign. Ph.D. Thesis. **1996**.

von Gunten, U.; Hoigne, J. Bromate formation during ozonization of bromide-containing waters: interaction of ozone and hydroxyl radical reactions. *Environ. Sci. Technol.* **1994**, *28* (7), 1234-1242.

von Gunten, U.; Oliveras, Y. Kinetics of the reaction between hydrogen peroxide and hypobromous acid: implication on water treatment and natural systems. *Water Res.* **1997**, *31* (4), 900-906.

Wajon, J. E., Morris, J. C. Rates of formation of N-bromo amines in aqueous solution. *Inorganic Chemistry*, **1982**, *21*(12), 4258-4263.

Wagner, E. D., Plewa, M. J. CHO cell cytotoxicity and genotoxicity analyses of disinfection by-products: an updated review. *J. Environ. Sci.* **2017**, *58*, 64-76.

Wang, W. L., Chen, Z., Du, Y., Zhang, Y. L., Zhou, T. H., Wu, Q. Y., Hu, H. Y. Elimination of isothiazolinone biocides in reverse osmosis concentrate by ozonation: A two-phase kinetics and a non-linear surrogate model. *J. Hazard. Mater.* **2020**, *389*, 121898.